Royal Netherlands
Meteorological Institute
Ministry of Infrastructure
and Water Management

Validation of hourly precipitation extremes in the Regional Atmospheric Climate Model (RACMO) for the Netherlands and surrounding regions

Sebastiaan de Haas

De Bilt, 2025| Technical report; TR 25-04

Royal Netherlands
Meteorological Institute
Ministry of Infrastructure
and Water Management

WAGENINGEN UNIVERSITY
METEOROLOGY AND AIR QUALITY

M.Sc. Climate Studies

Specialization: The Physical Climate System

Research internship report

Validation of hourly precipitation extremes in the Regional Atmospheric Climate Model (RACMO) for the Netherlands and surrounding regions

---

by

Sebastiaan de Haas

March 6, 2025

Supervisors KNMI:
Leon van Voorst MSc & Dr. Henk van den Brink

Supervisor Wageningen University:
Prof. Jordi Vilà-Guerau de Arellano

Abstract

Hourly precipitation extremes in the Regional Atmospheric Climate Model (RACMO) are validated for the Netherlands and surrounding regions, primarily with the goal of assessing whether hourly extremes are sufficiently well represented in RACMO for its use in hydrological applications. This is done by a comparison to HARMONIE (in climate mode) at convection-permitting resolutions, and to observations from measurement stations within the Netherlands. Firstly, the spatial precipitation distribution in RACMO is assessed by comparing individual events of the largest hourly precipitation extremes in RACMO to the same events in HARMONIE. This comparison shows that precipitation in RACMO is substantially more clustered, is frequently spatially shifted and/or occurs over different regions compared to HARMONIE. Thereby, RACMO seems to misrepresent spatial precipitation patterns, although a comparison to observations is required to definitively conclude this. Furthermore, data pooling is used to validate return periods of hourly precipitation in RACMO by a comparison to HARMONIE and observations, from which we conclude that hourly precipitation extremes in RACMO up to return periods of $\sim$1000 years are too low. Conversely, for return periods of $\gtrsim$1000 years it seems that the hourly extremes in RACMO are too high, although more data from observations and HARMONIE is required to conclusively determine this. Finally, we validate the dew point temperature (T_{dew}) in RACMO due to its essential role in governing precipitation extremes, and compare the effect of T_{dew} on hourly precipitation extremes between RACMO, HARMONIE and the observations. Based on this evaluation, we conclude that the T_{dew} mean and distribution in RACMO compare well to the observations, while RACMO overestimates the T_{dew} extremes. Finally, the effect of T_{dew} on hourly precipitation extremes differs considerably between RACMO and both HARMONIE and the observations. Based on the results presented in this report, we believe that RACMO generally does not perform well in reproducing hourly precipitation extremes, and that the misrepresentation of spatial precipitation patterns during hourly extreme events is especially problematic when RACMO is adopted for hydrological applications.

Contents

Chapter 1

Introduction & motivation

Extreme precipitation events have frequently caused severe riverine flooding in Europe over the last decades, often resulting in substantial socio-economic costs and in some cases also casualties (Paprotny et al., 2024). A fraction of extreme precipitation events occur on hourly timescales, and can result in flash flooding. These are caused by convective rainfall events that occur locally, and which can significantly impact basins up to 1000 km^2 (Marchi et al., 2010). These basins can then respond and flood within a few hours or less, occasionally leading to heavy socio-economic losses. An example of an extreme flash flood in Europe that was particularly damaging is the June 2008 event in South-West Germany (Ruiz-Villanueva et al., 2012). Intense convective rainfall poured over the catchment of a small creek, recording e.g. 107 mm of precipitation in one hour (based on radar observations) and causing extreme discharge that resulted in substantial damage to buildings and infrastructure. A very recent extreme flash flooding event occurred in the Valencia region of Spain during October 2024, recording 491 mm of precipitation in 8 hours and causing over 200 casualties (World Meteorological Organization, https://wmo.int/media/news/devastating-rainfall-hits-spain-yet-another-flood-related-disaster). Worryingly, flash floods in central and western Europe have increased in frequency over the last few decades (Meyer et al., 2021).

Precipitation extremes on hourly timescales are therefore important for hydrological applications such as flooding and river discharge. Investigating hydrological extremes requires information on return periods of the largest precipitation extremes. This in turn requires long series of precipitation data, however, observational data sets are too short for getting sufficient statistics on precipitation extremes. One solution is using climate models to obtain long periods of simulation data, where one such model is the Regional Atmospheric Climate Model (RACMO, van Meijgaard et al., 2008) at 0.11 degrees (∼12 x 12 km) resolution. Daily precipitation extremes in RACMO have already been assessed on sub-catchment scale in the Meuse by van Voorst and van den Brink (2023), however, hourly extreme precipitation has not yet been validated and are essential for smaller catchments due to their quick response times, as mentioned. As the resolution of RACMO is insufficient for resolving convection (thereby using parameterized convection), extreme hourly precipitation events and their spatial distribution are likely difficult to reproduce as these predominantly originate from summertime convective storms (Lenderink et al., 2021). When using precipitation data of extreme events for hydrological applications, the spatial distribution of precipitation is especially important and thereby also essential to validate, in addition to the statistics of extreme precipitation. Thereby, a thorough validation of RACMO in

terms of its capacity to reproduce spatial and statistical patterns of hourly precipitation extremes is required to assess its reliability for hydrological applications.

Dew point temperature (T_{dew}) has been shown to be an essential metric for hourly precipitation extremes (Lenderink et al., 2011). Dew point temperature is the temperature that air needs to be cooled down to at constant pressure to become fully saturated, i.e. obtain a relative humidity of 100%. A large T_{dew} is thereby a combination of a large temperature and high relative humidity. When T_{dew} is high, extreme convective storms may develop due to the combination of moist air and potential for intense convection, which in turn may cause large hourly precipitation extremes (albeit requiring additional atmospheric conditions). In Beersma, Versteeg, and Hakvoort (2018), it is shown that the largest hourly precipitation extremes are very sensitive to T_{dew} based on station data in the Netherlands, where hourly precipitation data with $T_{\text{dew}} > 17.5$ °C show significantly more frequent occurrence of the largest precipitation extremes compared to precipitation data with $T_{\text{dew}} < 17.5$ °C. The dew point temperature and its extremes are therefore also validated in RACMO, including their effect on precipitation extremes.

Chapter 2

Methodology

2.1 Available data

We use RACMO (version 2.3, cycle 33) reanalysis data between 2008-2021 at 0.11 degrees (∼12 x 12 km) resolution, where the implemented parameterizations in this RACMO version are based on ECMWF-IFS (European Center for Medium-range Weather Forecast - Integrated Forecasting System) CY33R1 (ECMWF, 2009). RACMO is forced by ERA (ECMWF reanalysis) interim (Berrisford et al., 2009) between 2008-2018 and by ERA5 (Hersbach et al., 2020) for 2019-2021. We use a similar reanalysis product for the HARMONIE model (in climate mode, cycle 38, Belušić et al., 2020), with higher resolution (2.5 x 2.5 km) and slightly smaller domain compared to RACMO. The domains of RACMO and HARMONIE (including the orographic height) are shown in fig 2.1. The forcing of HARMONIE is performed by RACMO reanalysis. No data assimilation has been used in both HARMONIE and RACMO. Furthermore, we have post-processed the HARMONIE reanalysis data to the RACMO grid to account for the effect of grid size (area) on values of precipitation extremes. It has been shown that if precipitation extremes are assessed over larger areas, the values of the extremes are reduced significantly (e.g., Overeem et al., 2010). Note that the HARMONIE data has been regridded to the RACMO domain during post-processing, so the HARMONIE reanalysis product is not re-run with different resolution. The regridding has been performed using conservative remapping from the climate data operators (CDO) software (Schulzweida, Kornblueh, and Quast, 2019). From now on this data is referred to as "HARMONIE regridded".

Furthermore, we have long simulation periods of RACMO from the KNMI-14 scenarios (version 2.1, Attema et al., 2014) and KNMI-23 scenarios (version 2.3, Van Dorland et al., 2023), both also at a resolution of 0.11 degrees. We use 16 ensemble members of historical KNMI-14 RACMO data forced by EC-Earth (model version 2.2, Hazeleger et al., 2012), between 1949-2013. The RACMO data from the KNMI-23 scenarios is also composed of 16 ensemble members and forced by EC-Earth (model version 3, Döscher et al., 2021), in this case for the historical period 1952-2020.

The model reanalysis data is primarily used for comparing individual extreme events of hourly precipitation in RACMO to the same events in HARMONIE, especially focusing on the spatial distribution of precipitation (and also time evolution with animations). The long simulation periods of RACMO from the KNMI-14 and KNMI-23 scenarios are used to evaluate the statistics (return periods) of extreme precipitation events.

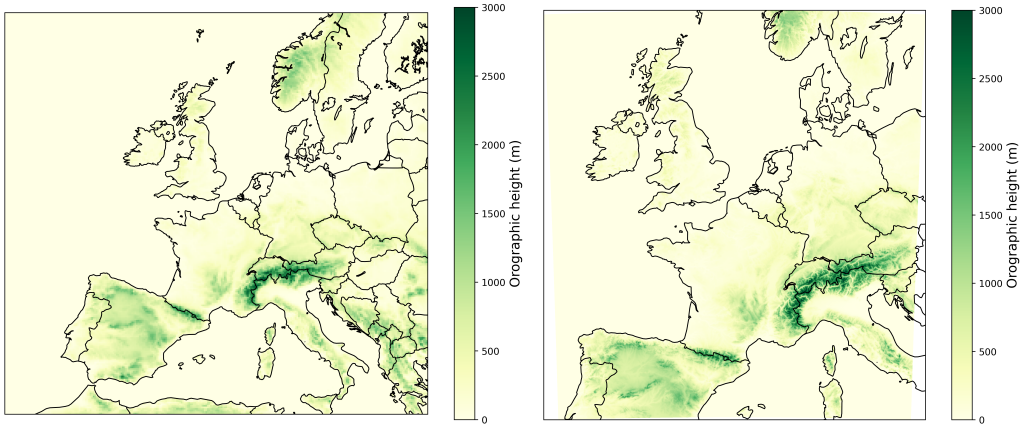

FIGURE 2.1: The full domains of RACMO (left) and HARMONIE (right) reanalysis, showing the orographic height in meters.

We exclusively use historical simulation periods for all models, and therefore do not consider climate change effects in this study.

Finally, we use precipitation data between 1991 and mid-2024 collected by 33 Automatic Weather Stations that are spread reasonably evenly over the Netherlands (Van Dorland et al., 2023). This observational data is only used to assess the statistics of extreme events, and therefore not for the spatial distribution and/or time evolution of extreme hourly precipitation events.

2.2 Data pooling

For assessing the return periods of hourly precipitation extremes between the different models and observations, data pooling has been used. This method combines precipitation data from different locations (in this case measurement stations or model grids) into a single data set, thereby obtaining return periods of extreme precipitation events that are longer by orders of magnitude. For example, when 10-year simulation runs with 100 grid cells are combined using data pooling, maximum return periods of 1000 years can be obtained. For this example, we are pretending that we have a single grid with a model run of 1000 years, therefore this method assumes that the precipitation data is independent and subjected to the same climatology. Although the latter assumption is (largely) valid when pooling over small regions such as the Netherlands, the former is violated when combining data from neighboring grid cells or nearby measurement stations. However, despite one or both of these assumptions typically being violated when using this method, data pooling is common practice in assessing precipitation extremes (e.g., Lenderink and Van Meijgaard, 2008) and has been shown to be robust even when pooling over neighboring model grid cells (e.g., Kendon et al., 2008).

Chapter 3

Results & discussion

In this chapter, results on hourly precipitation extremes in RACMO are presented and compared to HARMONIE and/or observations, and the results are discussed. In section 3.1, spatial patterns of hourly precipitation extremes in RACMO are compared to HARMONIE by verifying annual hourly precipitation extremes per grid and by comparing the spatial precipitation distribution of individual extreme events. In section 3.2, the return periods of hourly precipitation in RACMO are compared to HARMONIE and observations within the Netherlands. In section 3.3, the dew point temperature and its effect on extreme hourly precipitation in RACMO is again compared to HARMONIE and observations within the Netherlands. Finally, note that as explained in section 2.1, HARMONIE regridded in this work refers to HARMONIE output post-processed to the RACMO grid, therefore HARMONIE has not been run separately with different grid and resolution. The regridding of HARMONIE has been performed only to account for the area effect on values of precipitation extremes (e.g., Overeem et al., 2010).

3.1 Spatial assessment of hourly precipitation extremes

In this section, the spatial precipitation distribution and its time evolution in RACMO is compared to HARMONIE, as the latter is more likely to capture spatial precipitation patterns due to its convection-resolving resolutions. Despite our results in section 3.2 and 3.3 showing good agreement between HARMONIE and the observations for hourly precipitation and dew point temperature statistics, we did not validate HARMONIE in terms of spatial distribution of precipitation. Therefore, we mention two papers that have assessed the performance of HARMONIE in simulating spatial patterns of extreme hourly precipitation. Firstly, in Xie et al. (2024), the annual hourly (and also daily) precipitation extremes in HARMONIE (also in climate mode and for cycle 38) have been compared spatially to observations at 3 km and 12 km resolution in Norway. This was done to assess the effect of convection-permitting resolutions versus parameterized convection in HARMONIE on the quality of precipitation extremes. The annual hourly precipitation extremes in HARMONIE at 3 km resolution show significantly less bias compared to the 12 km resolution runs throughout most of Norway ($\sim$1.5 mm bias on average for 3 km resolution compared to $\sim$4 mm at 12 km). Secondly, Attema, Loriaux, and Lenderink (2014) compare the spatial distribution of a single extreme hourly event (peaking at 67 mm/h) in the Netherlands in HARMONIE (again in climate mode, cycle 37) to a combination of radar and ground-based observations. They conclude that although the shower location shifted slightly, the spatial precipitation distribution in HARMONIE compares reasonably

well with the observations, especially considering that no data assimilation is used. Despite both papers providing some confidence in the ability of HARMONIE to reproduce spatial patterns of hourly precipitation extremes, we note that the verification in both papers is limited, and additionally that the former study was performed in Norway where precipitation is largely orographic. Therefore, the comparison of RACMO to HARMONIE in this section should be regarded as a first step towards validating the spatial distribution of hourly precipitation extremes in RACMO, and an additional comparison to observations is recommended as future research (see section 4.2).

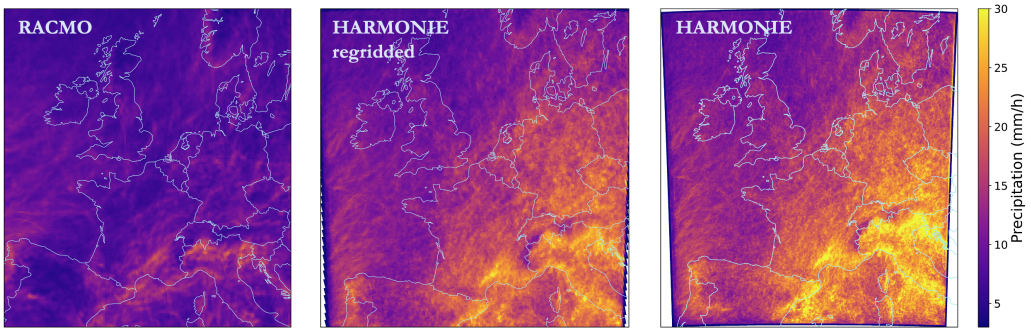

FIGURE 3.1: Annual maximum hourly precipitation per grid averaged over each year between 2008-2021 for RACMO reanalysis (left panel), HARMONIE regridded (middle panel) and HARMONIE (right panel).

In Fig. 3.1, the averaged annual maximum hourly precipitation per grid is shown for RACMO reanalysis (left panel), HARMONIE regridded (middle panel) and HARMONIE (right panel). The figure displays the largest hourly precipitation that occurs within each year for every grid individually, averaged over 2008-2021. The figure shows that annual hourly precipitation extremes in RACMO are considerably lower compared to HARMONIE throughout the domain. When comparing RACMO to HARMONIE regridded and thereby accounting for the grid area difference between the models, the discrepancies are lower but still substantial. The regions where the largest annual hourly precipitation extremes occur within the domains do roughly correspond between RACMO and HARMONIE (mostly around the Alps and Southern Europe).

In Fig. 3.2, the cumulative 48-hour precipitation for three of the largest hourly precipitation extremes in RACMO are compared to the same events in HARMONIE, and also the post-processed HARMONIE regridded, for the 24 hours before and after the hourly extreme occurred. In the upper panels, the second largest hourly precipitation event is compared, and the middle and lower panels show the fifth and tenth largest hourly extreme events in RACMO, respectively. These events have been chosen only because the remaining seven of the ten largest hourly precipitation extremes in RACMO are not located within the HARMONIE domain. Also, a large fraction of the second highest hourly extreme event in RACMO evolves outside of the HARMONIE domain. Comparing these hourly extremes in RACMO to the same events in HARMONIE and HARMONIE regridded in Fig. 3.2, two differences in terms of spatial distribution of precipitation between the models stand out. Firstly, RACMO shows narrow bands of extreme precipitation, which are most pronounced for the number two and five largest hourly extremes in the upper and

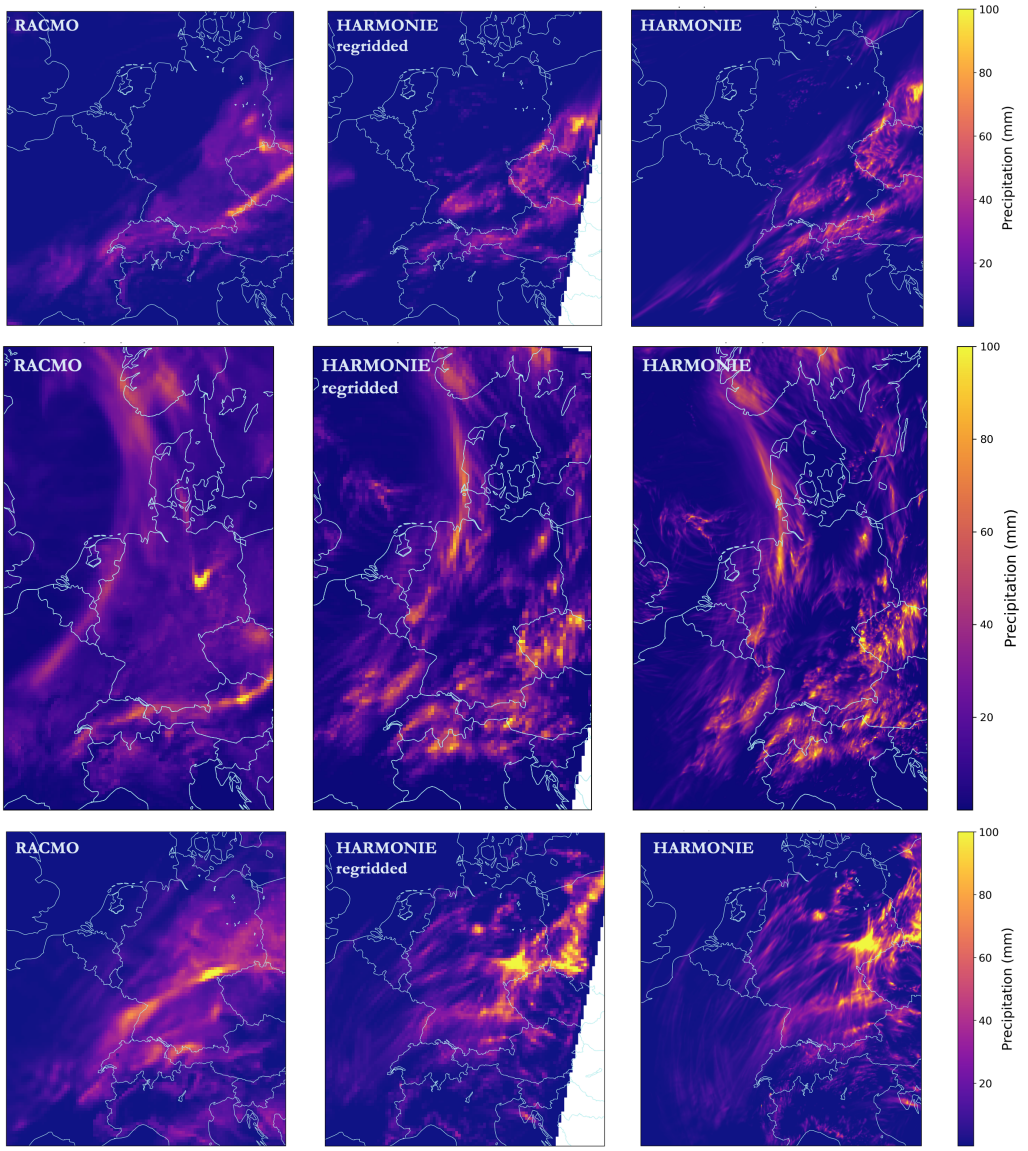

FIGURE 3.2: The cumulative 48-hour precipitation for three of the largest hourly extreme events in RACMO reanalysis (upper, middle and lower panels, summed over the 24 hours before and after the occurrence of the maximum hourly extreme). These events in RACMO reanalysis (left panels) are compared to the same events in HARMONIE regridded (middle panels) and HARMONIE (right panels).

middle panels. These narrow precipitation bands are caused by one or a few large aggregated systems with high precipitation rates, and occur more frequently in RACMO (this is further discussed in the next paragraph). In HARMONIE, precipitation patterns are substantially different compared to RACMO, primarily being more spatially distributed. Also, locations with high precipitation volumes are typically shifted or occur over entirely different regions when comparing HARMONIE and RACMO. This is well reflected in the

fifth largest hourly extreme event of RACMO (second row in Fig. 3.2), where the curved precipitation band that occurs over the middle-left of the model domains (partially over the Dutch-German border in RACMO) is shifted to the right in HARMONIE compared to RACMO. Additionally, RACMO contains an area with large precipitation volumes in Germany which is not reflected in HARMONIE, and RACMO also exhibits significantly reduced precipitation volumes and different precipitation patterns compared to HARMONIE in the Czech Republic. These are examples to illustrate the difference in spatial patterns of extreme precipitation between RACMO and HARMONIE, and similar discrepancies occur for the other two events shown in Fig. 3.2.

In Fig. 3.3, the tenth largest hourly extreme event of RACMO is shown at 17:00, 19:00, 21:00 and 23:00 UTC, including contours of the sea level pressure anomaly (SLPA) which are given by the sea level pressure subtracted by the yearly-averaged sea level pressure. In Fig. 3.4, the same extreme event is shown for HARMONIE at 16:30, 18:30, 20:30 and 22:30, again including contours of SLPA which for these figures are given by the sea level pressure subtracted by the monthly-averaged sea level pressure. The time in HARMONIE deviates from RACMO by 30 minutes for precipitation, however, for SLPA this is not the case. Therefore, in Fig. 3.4, the precipitation and SLPA times also differ by 30 minutes. Additionally, even though the year-averaging for RACMO and month-averaging for HARMONIE in determining SLPA likely contributes significantly to the deviating SLPA values between the two models, the SLPA contours are merely included for assessing whether the extreme precipitation is driven by a low pressure system. The SLPA contours indicate that this seems to be the case for this event. Note also that this event occurred on 2021-07-16, which is shortly after the extreme precipitation event of 13-15 July in a similar area that resulted in more than 200 casualties and exceptional economic damage (estimated $\gtrsim$5 billion euros) from riverine flooding (Kreienkamp et al., 2021). When comparing this extreme hourly event in RACMO to HARMONIE, systems with high precipitation rates are smaller and more spatially distributed in HARMONIE, as also reflected in the lower panels of Fig. 3.2. The time evolution of this event in RACMO does show that the narrow precipitation band over Germany in the lower-left panel of Fig. 3.2 is caused by several organized systems. For the second largest hourly extreme event in RACMO, the narrow band of extreme precipitation that occurs in the upper-left panel of Fig. 3.2 primarily originates from a single organized system that produces high precipitation rates ($\gtrsim$30 mm/h) over multiple grids for a period of more than 24 hours. Four time steps of this event in RACMO are shown in appendix Fig. 5.6. It is not compared to HARMONIE as we believe this event to show unrealistically persistent (>24 hours) rates of high precipitation.

The substantial difference in spatial precipitation distribution and its evolution over time between RACMO and HARMONIE serves as a strong indication that RACMO is unable to produce realistic spatial patterns of extreme hourly precipitation. This is especially problematic when RACMO is adopted for hydrological applications. To conclusively determine the reliability of spatial patterns in RACMO would require a spatial comparison of hourly extreme events to observations, however, based on the results presented in this section we believe RACMO performs poorly in simulating spatial distributions of hourly extreme precipitation. As a final note, the spatial precipitation distribution seems to improve when switching off the convection scheme and running RACMO with a resolution of 6 x 6 km. Although this resolution is insufficient to resolve convection, this is an indication that the extreme precipitation that seems too clustered in RACMO may be caused by the

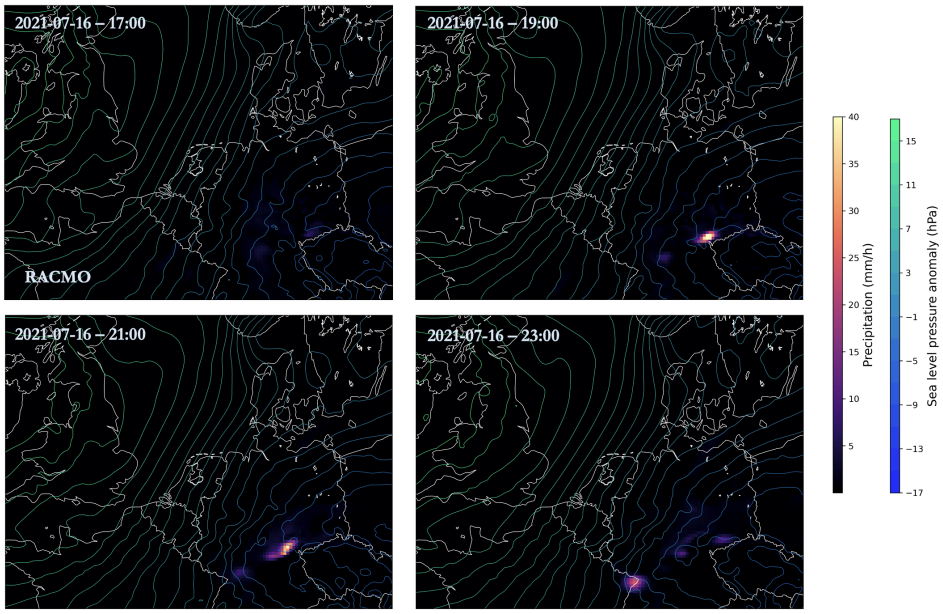

FIGURE 3.3: Four time steps of the tenth largest hourly extreme precipitation event in RACMO (same event as the lower panels of Fig. 3.2) at 17:00, 19:00, 21:00 and 23:00 UTC. The contours represent the sea level pressure (SLP) anomaly, given by the SLP subtracted by the yearly-averaged SLP.

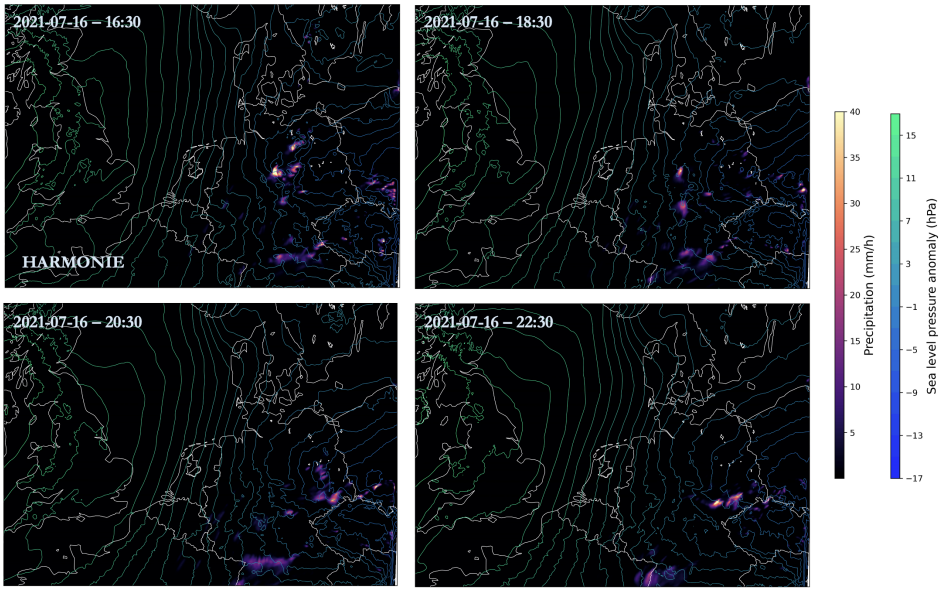

FIGURE 3.4: Same extreme event as Fig. 3.3 shown in HARMONIE (also the same event as the lower panels of Fig. 3.2), shown at 16:30, 18:30, 20:30 and 22:30 UTC. The contours represent the sea level pressure (SLP) anomaly, given by the SLP subtracted by the monthly-averaged SLP. The SLP and precipitation contain 30-minute time differences.

convection scheme.

3.2 Return period comparison of hourly precipitation extremes

In Fig. 3.5, return periods of hourly precipitation are shown for observations, RACMO reanalysis, HARMONIE, HARMONIE regridded, and RACMO from both the KNMI-14 and KNMI-23 scenarios. Data pooling has been used for creating this figure, which is explained in section 2.2 including the limitations and assumptions of this method. In short, precipitation data of model grid cells or observation stations within the Netherlands are combined into a single data set to create long precipitation series with large return periods. For example, combining the observational data from 33 stations with ∼30 years of data results in ∼990 years of data, which roughly corresponds to the largest return period for the observations in Fig. 3.5 (black line).

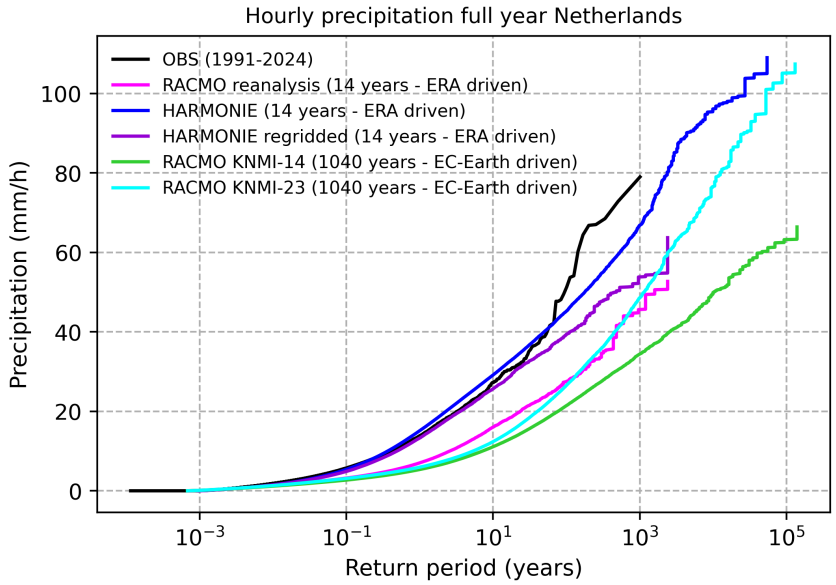

FIGURE 3.5: The return period of hourly precipitation between 2008-2021 for RACMO reanalysis (magenta), HARMONIE (blue), HARMONIE regridded (purple) all forced with ERA, and for 16 ensemble members between 1949-2013 for RACMO from the KNMI-14 scenarios (green) and 16 ensemble members from 1952-2020 for RACMO from the KNMI-23 scenarios (cyan) both forced with EC-Earth3, and finally for station observation data between 1991 and mid-2024 (black).

For the observations, it's important to note that the effect of area on precipitation extremes has not been accounted for in the comparison to RACMO and HARMONIE. When attempting to use areal reduction factors from Overeem et al. (2010) to take this into account, the precipitation extremes were too low. This is due to areal reduction factors from Overeem et al. (2010) only being available for two return periods (two and thirty years), meaning that we needed to fit the areal reduction factor as a function of return period based on these two values. This resulted in an unrealistic function, especially for large return periods. Therefore, areal reduction factors have not been used in the return period

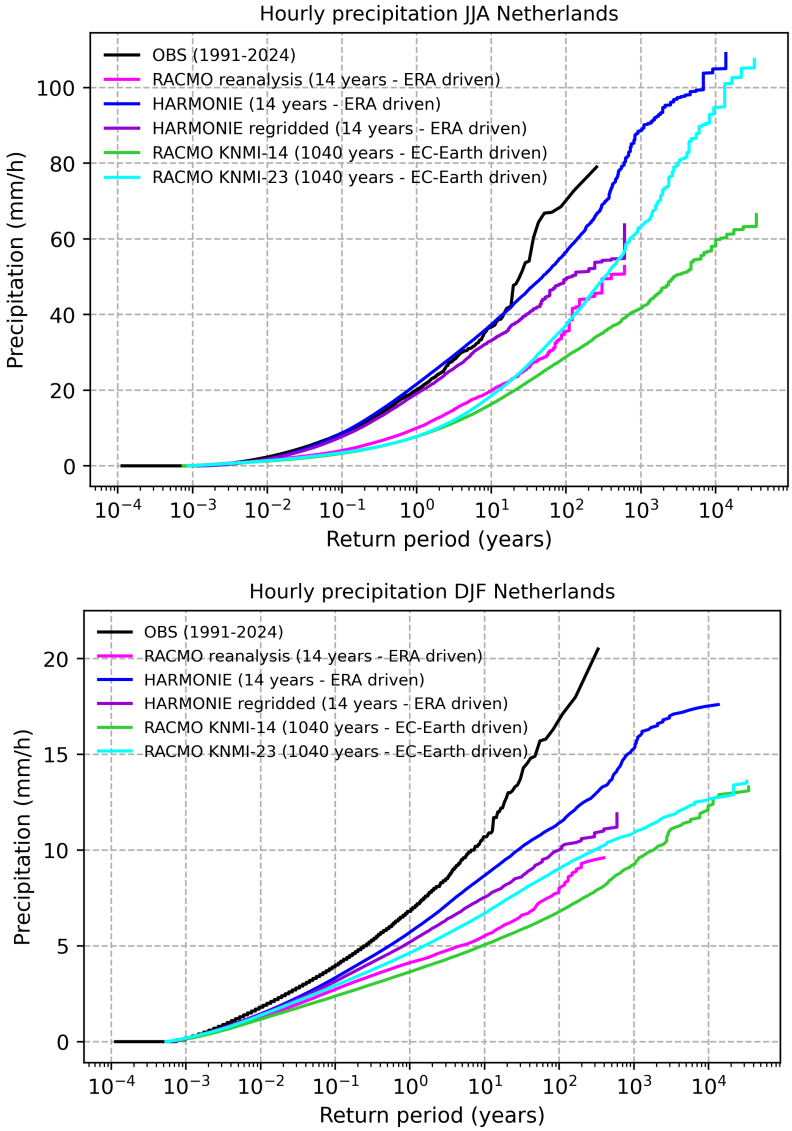

FIGURE 3.6: The return period of hourly precipitation for June, July and August (JJA, upper panel) and December, January and February (DJF, lower panel) between 2008-2021 for RACMO reanalysis (magenta), HARMONIE (blue), HARMONIE regridded (purple) forced with ERA, and for 16 ensemble members between 1949-2013 for RACMO from the KNMI-14 scenarios (green) and 16 ensemble members from 1952-2020 for RACMO from the KNMI-23 scenarios (cyan) both forced with EC-Earth3, and finally for station observation data between 1991 and mid-2024 (black).

figures of hourly precipitation in this chapter. When comparing RACMO to the observations, the latter curve would thereby have been significantly lower if area was accounted for, especially for larger precipitation extremes. Despite this limitation, RACMO reanalysis still shows precipitation extremes that are too small compared to the observations for

this return period range. Comparing the HARMONIE and HARMONIE regridded curves shows that accounting for area indeed reduces the precipitation extremes significantly.

When comparing HARMONIE to the observations, where the effect of area on precipitation extremes is reduced due to HARMONIE's high resolution, the two curves compare very well except for the largest hourly extremes. However, the tails of the hourly precipitation distributions suffer from low statistics, therefore the high-return period parts of the curves may look very differently if more data would be included. Therefore, we conclude that HARMONIE performs well in reproducing return periods of extreme hourly precipitation.

The RACMO reanalysis hourly precipitation extremes are also lower than HARMONIE regridded. However, for the largest return periods towards the end of the curve, RACMO becomes steeper compared to HARMONIE regridded. From the curves it seems that if more precipitation data would be available, the hourly extremes in RACMO may exceed HARMONIE for return periods above $\sim 10^3$ years. We have therefore included longer time-series of RACMO precipitation data from the KNMI-14 and KNMI-23 scenarios, despite not having longer series of HARMONIE data. For RACMO from the KNMI-23 scenarios, the curve is very similar to RACMO reanalysis and indeed exceeds HARMONIE regridded for high return periods. It seems that if more HARMONIE data was available, the HARMONIE regridded curve would remain below the RACMO curve for return periods of $\gtrsim 10^3$ years, although this is uncertain. Despite this uncertainty, we hypothesize that the RACMO hourly precipitation extremes are too high for these large return periods. For RACMO KNMI-14, the hourly precipitation is substantially lower compared to the other curves throughout the full return period range. This is likely caused by unrealistically low dew point temperatures from the forcing by EC-Earth (version 2.2), as discussed in section 3.3.

In Fig. 3.6, the hourly precipitation vs return period is shown for June-July-August (JJA, upper panel) and December-January-February (DJF, lower panel) separately. The JJA panel looks very similar to Fig. 3.5, meaning that the largest hourly precipitation extremes occur during these months for all displayed models and for the observations. During DJF, the hourly precipitation extremes are substantially lower. Despite the models showing better agreement for these months, the differences are still significant and the discrepancy with the observations is large for all models (although again the observations curve should be lower to account for the differences in area). As the largest hourly precipitation extremes occur during the summer months JJA, we will focus on this period when assessing dew point temperature and its effect on extreme hourly precipitation in the next section.

3.3 Dew point temperature and its effect on hourly precipitation extremes

As explained in the introduction, the dew point temperature (T_{dew}) is a measure of both temperature and relative humidity, and therefore important for precipitation and precipitation extremes. In the upper panel of Fig. 3.7, the normalized probability distribution function (PDF) is shown for the Netherlands during JJA for RACMO reanalysis, HARMONIE, HARMONIE regridded, RACMO from both the KNMI-14 and KNMI-23 scenarios and the observations. In the lower panel of Fig. 3.7, the return period of T_{dew} is shown for the same models and observations, again during JJA and within the Netherlands. Also,

the corresponding means and standard deviations of the PDFs are listed in table 3.1. For HARMONIE, T_{dew} was calculated using the Magnus-Tetens formula, which is given by

$$T_{\text{dew}} = (b\alpha(T, \text{RH}))/(a - \alpha(T, \text{RH})), \tag{3.1}$$

where

$$\alpha(T, \text{RH}) = ln(\text{RH}/100) + aT/(b + T), \tag{3.2}$$

$a = 17.625$ and $b = 243.04$ °C (Lawrence, 2005). The equation is valid for temperatures between -40 and 50 °C, and the uncertainty in T_{dew} is 0.35 °C. For all RACMO data and the observations, T_{dew} is available as standard output. Therefore, note that dew point temperature may have been inferred based on different equations.

	T_{dew} mean (°C)	T_{dew} std dev (°C)
Observations	13.04	3.06
RACMO reanalysis	12.66	3.15
HARMONIE	12.03	3.25
HARMONIE regridded	12.11	3.22
RACMO KNMI-14	10.53	2.92
RACMO KNMI-23	12.08	3.16

TABLE 3.1: The dew point temperature (T_{dew}) mean and standard deviation (std dev). The corresponding probability distribution functions (normalized) are shown in Fig. 3.7.

The T_{dew} PDF, mean and standard deviation of RACMO reanalysis and the observations all show good agreement with the observations during JJA and within the Netherlands. However, the T_{dew} return period figure shows that the extremes in RACMO reanalysis are significantly larger compared to the observations. For HARMONIE and HARMONIE regridded, the mean T_{dew} is ∼1 degree too low and also the PDF is shifted to smaller T_{dew} values compared to the observations, however, the T_{dew} extremes show excellent agreement.

For RACMO from the KNMI-23 scenarios, the mean T_{dew} is ∼1 degrees lower compared to the observations, and the extremes (return period figure in the lower panel of Fig. 3.7) are again too large compared to the observations, similar to RACMO reanalysis. For RACMO from the KNMI-14 scenarios, the mean T_{dew} is ∼2.5 degrees too low compared to the observations, and also the T_{dew} extremes are substantially lower. Therefore, the properties of T_{dew} between RACMO reanalysis and RACMO from the KNMI-23 scenarios is very similar, while for RACMO from the KNMI-14 scenarios the T_{dew} shows consistently too low values (caused by the forcing from EC-Earth version 2.2). This is in line with the hourly precipitation extremes in Fig. 3.5, which are also similar between RACMO reanalysis and RACMO KNMI-23, while displaying lower extremes for RACMO KNMI-14. This is a strong indication that T_{dew} is at least partially dictating the hourly precipitation extremes in RACMO.

Therefore, we explore the effect of T_{dew} on hourly precipitation. We do this by separating the hourly precipitation return period curves between precipitation where $T_{\text{dew}} > 17.5$ and $T_{\text{dew}} < 17.5$ °C, shown in Fig. 3.8. As explained in the last paragraph of the introduction,

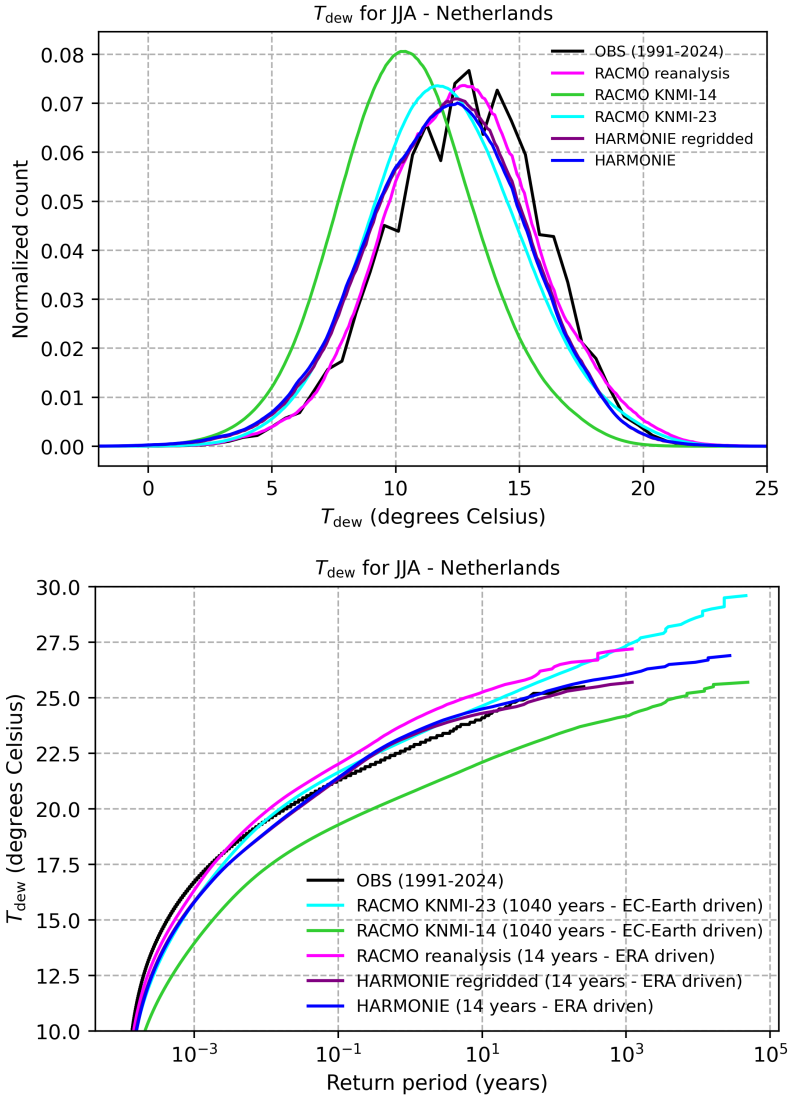

FIGURE 3.7: The normalized probability distribution function (PDF, upper panel) and return period (lower panel) of dew point temperature (T_{dew}) for June, July and August (JJA) between 2008-2021 for RACMO reanalysis (magenta), HARMONIE (blue), HARMONIE regridded (purple) forced with ERA, and for 16 ensemble members between 1949-2013 for RACMO from the KNMI-14 scenarios (green) and 16 ensemble members from 1952-2020 for RACMO from the KNMI-23 scenarios (cyan) both forced with EC-Earth3, and finally for station observation data between 1991 and mid-2024 (black).

it has been shown with observations that the two curves look very similar for return periods up to ∼50 years, but very differently for return periods of $\gtrsim$50 years. The curve with $T_{dew} > 17.5$ °C then becomes substantially steeper compared to the one with $T_{dew} < 17.5$ °C, thereby displaying two "populations" of precipitations vs return period (Beersma, Versteeg, and Hakvoort, 2018). In both panels of Fig. 3.8, we now show probability of

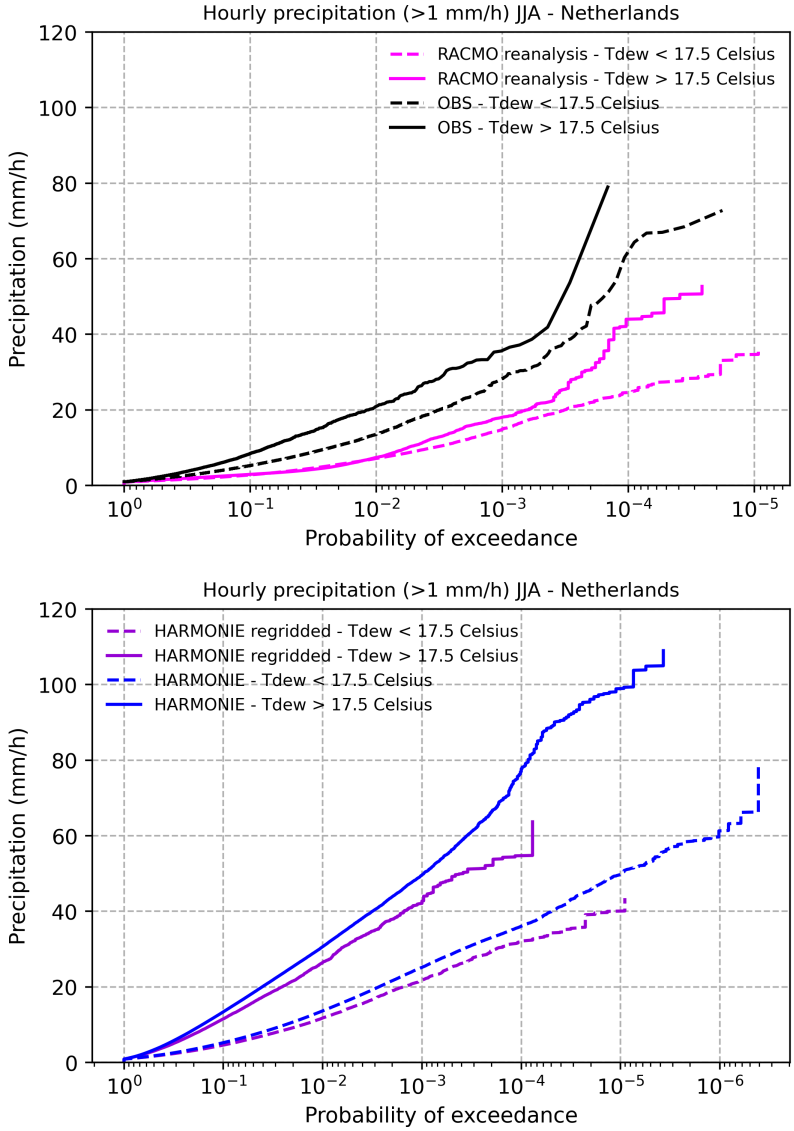

FIGURE 3.8: The hourly precipitation for dew point temperatures $T_{\mathrm{dew}} > 17.5$ °C (solid curves) and $T_{\mathrm{dew}} < 17.5$ °C (dashed curves) during June, July and August (JJA) for station observation data between 1991 and mid-2024 (black, upper panel) and between 2008-2021 for RACMO reanalysis (magenta, upper panel), HARMONIE (blue, lower panel) and HARMONIE regridded (purple, lower panel).

exceedance rather than return period as only precipitation with values > 1 mm/h are included, however both quantities are very similar.

The RACMO reanalysis curves in the upper panel of Fig. 3.8 displays the aforementioned two populations of hourly precipitation extremes, where the curves look very similar up to a probability of exceedance of $\sim 5 \times 10^3$ and very distinct afterwards. This highlights

the sensitivity of precipitation extremes in RACMO to dew point temperature, where precipitation rates of $\gtrsim$ 20 mm/h occur considerably more frequently when T_{dew} is larger than 17.5 °C. The observations (black curves in upper panel of Fig. 3.8) also show this, but not as pronounced. Namely, the observational curve with $T_{\text{dew}} < 17.5$ °C also exhibits a steeper trend for low probabilities of exceedance (so large return periods), albeit to a lesser degree and at slightly lower probabilities of exceedance than the curve with $T_{\text{dew}} > 17.5$ °C.

In HARMONIE and HARMONIE regridded, two very different populations of hourly precipitation extremes separated by dew point temperature occur, as shown in the lower panel of Fig. 3.8. However, the two populations vary substantially from RACMO and the observations, and those found in Beersma, Versteeg, and Hakvoort (2018). For HARMONIE, the two curves separated by T_{dew} already deviate at very large probabilities of exceedance (low return periods), and do not show the increase in steepness for the lowest probabilities of exceedance. Therefore, hourly precipitation extremes in HARMONIE respond very differently to T_{dew} compared to both RACMO and the observations. However, the two populations of hourly precipitation extremes as in Beersma, Versteeg, and Hakvoort (2018) may also occur in HARMONIE if another threshold than 17.5 °C for T_{dew} is chosen.

To further investigate the difference in relation between hourly precipitation extremes and T_{dew}, and to infer if hourly precipitation extremes in HARMONIE indeed respond sensitively to T_{dew} at another threshold, we plot the precipitation-T_{dew} distribution in Fig. 3.9 for RACMO reanalysis, HARMONIE regridded and the observations again during JJA and for Netherlands. The number of counts within a certain precipitation and T_{dew} range is indicated with a color. For RACMO reanalysis, the precipitation-T_{dew} distribution is similar when separated by a T_{dew} of 17.5 °C, except for the largest extremes which all occur above this threshold, as also reflected in Fig. 3.8. Furthermore, for the most extreme dew point temperatures ($T_{\text{dew}} \gtrsim 22.5$ °C), RACMO reanalysis only shows low hourly precipitation rates. However, this is likely due to the low occurrence of T_{dew} extremes, in addition to other conditions being required for intense hourly precipitation (e.g. large convective available potential energy). For HARMONIE regridded, the threshold for the largest hourly precipitation extremes seems to be located around $T_{\text{dew}} \sim 16$ °C, and for the observations many of the largest hourly precipitation extremes occur even substantially below dew point temperatures of 17.5 °C. The precipitation-T_{dew} distributions in Fig. 3.9, in combination with the T_{dew} separated return period curves for hourly precipitation in Fig. 3.8 therefore imply that the response of hourly precipitation extremes to T_{dew} is significantly different between RACMO reanalysis, HARMONIE regridded and the observations. However, as the largest precipitation extremes are based on low statistics, the figures presented in this section may look very different if more precipitation data would have been available, which is also shortly discussed in the next paragraph. Despite this constraint, these and the other results presented in the chapter imply that one or more processes underlying extreme hourly precipitation in RACMO are not well captured, which as mentioned likely includes convection. However, drawing this conclusion would require further research on convective properties of extreme precipitation in RACMO.

The precipitation-T_{dew} distribution is also shown for RACMO from the KNMI-23 and KNMI-14 scenarios in Fig. 3.10, again during JJA and within the Netherlands. However, for creating these figures, only two ensemble members (instead of 16) are included for

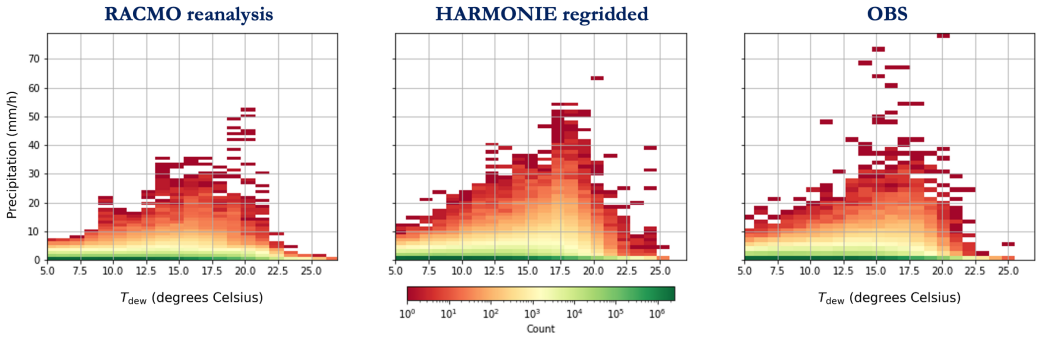

FIGURE 3.9: The hourly precipitation and dew point temperature (T_{dew}) distribution during June, July and August (JJA) between 2008-2021 for RACMO reanalysis (left panel), HARMONIE regridded (middle panel) and station observation data between 1991 and mid-2024 (right panel). The colors indicate the number of data points that fall within the corresponding precipitation and dew point temperature range.

each of the RACMO distributions, so ∼130 years of model data. For RACMO KNMI-23, the distribution is substantially different compared to RACMO reanalysis, despite the precipitation return period and T_{dew} PDF and return period curves being reasonably similar between RACMO reanalysis and RACMO KNMI-23 (see the upper panel of Fig. 3.6 and the lower panel of Fig. 3.7). As the same version of RACMO has been used for performing the reanalysis and KNMI-23 scenarios simulations, and only the forcing between them differs, this implies that the largest hourly precipitation extremes ($\gtrsim$ 40 mm/h) only occurring for $T_{dew} > 17.5$ °C in RACMO reanalysis is coincidental (possibly from only one or a few events) and caused by insufficiently long simulation data. For RACMO from the KNMI-14 scenarios, it seems that the dew point temperatures are too low for generating sufficiently large hourly precipitation extremes to draw a definitive conclusion on the effects of T_{dew} on hourly extremes. The lower T_{dew} in RACMO from the KNMI-14 scenarios is caused by the forcing of EC-Earth (version 2.2).

Return periods of hourly precipitation and dew point temperature are also presented for an extended domain (see appendix Fig. 5.1) in appendix Fig. 5.2 and Fig. 5.4, respectively. For the hourly precipitation, return period figures are also again shown separately for JJA and DJF in appendix Fig. 5.3. This analysis has been conducted to obtain larger return periods on hourly precipitation and dew point temperature, and to thereby assess the validity of the largest extremes in RACMO by a comparison to HARMONIE.

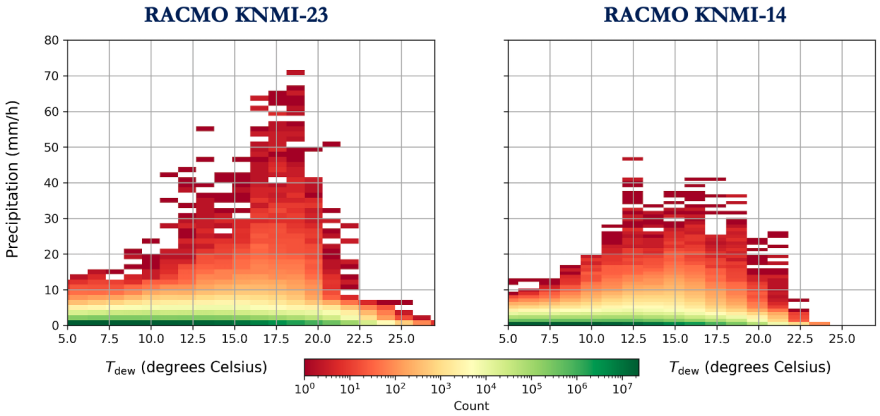

FIGURE 3.10: The hourly precipitation and dew point temperature (T_{dew}) distribution during June, July and August (JJA) for two ensemble members from 1952-2020 for RACMO from the KNMI-23 scenarios (left panel) and two ensemble members between 1949-2013 for RACMO from the KNMI-14 scenarios (right panel). The colors indicate the number of data points that fall within the corresponding precipitation and dew point temperature range.

Chapter 4

Conclusions and future research

4.1 Conclusions

We have validated extreme hourly precipitation in RACMO by comparison to HARMONIE (in climate mode and at convection-permitting resolutions) and observations, with the purpose of assessing whether hourly extremes in RACMO are sufficiently well represented for using the model in hydrological applications. The analysis is limited to the Netherlands, with the exception of spatial precipitation patterns, where also surrounding regions were included (see Fig. 5.1). This larger domain including surrounding regions have also been analyzed statistically, the results of which are included in the appendix.

Based on section 3.1, in which the spatial precipitation distribution and time evolution based on individual events are presented and discussed, we conclude that the spatial precipitation patterns in RACMO do not compare well to HARMONIE. Systems with high precipitation rates are too clustered in RACMO, are often shifted or occur over different regions compared to HARMONIE, and can be too long-lived (up to at least 24 hours of $\gtrsim$30 mm/h). As mentioned however, this is concluded based on a comparison to HARMONIE at convection-permitting resolutions, and therefore an additional comparison to observations is required to conclusively determine this. Despite this constraint, we believe that the aforementioned features of spatial precipitation patterns are likely misrepresented in RACMO and will cause issues when using the model for hydrological applications of extremes such as riverine flooding.

In section 3.2, return periods of hourly precipitation are presented and discussed based on data pooling (see section 2.2). From these results, we conclude that hourly precipitation extremes in RACMO are too low for return periods up to $\sim$1000 years. Conversely, hourly extremes seem too high in RACMO for return periods of $\gtrsim$1000 years, however, more precipitation data from observations and/or HARMONIE is required to definitively draw this conclusion. Furthermore, nearly all of the largest hourly precipitation extremes in RACMO, HARMONIE and the observations occur during summer (June, July, August). During winter (December, January, February), the return period curves between the models show less discrepancies, albeit still significant. However, in the return period figures, the effect of area on precipitation extremes has not been taken into account. Accounting for this would have significantly reduced the values of precipitation extremes for the observations when compared to RACMO, but despite this limitation and the assumptions that are implicitly made by using data pooling (see again section 2.2), we are reasonably confident in the conclusions mentioned in this paragraph.

The dew point temperature and its effect on hourly precipitation extremes are discussed in section 3.3. Here we find that the dew point temperature mean and distribution in RACMO compare well to the observations, while the dew point temperature extremes are too high. Furthermore, we have shown that hourly precipitation extremes respond differently to dew point temperature between RACMO, HARMONIE and the observations.

The results presented in this report imply that at least one physical process underlying extreme precipitation is not well captured by RACMO, which likely involves convection as discussed in the next section. Overall, RACMO does not perform well in reproducing hourly precipitation extremes, and especially the misrepresentation of spatial precipitation patterns is problematic when RACMO is used for hydrological applications.

4.2 Future outlook

To investigate the origin of the high degree of precipitation clustering in RACMO, the effect of convection on the organization of precipitation should be assessed. As mentioned, this has shortly been looked into (by Femke Brouwer) by comparing the spatial precipitation distribution in RACMO between parameterized convection at 12 km resolution and a switched-off convection scheme at 6 km resolution. However, this was only done for two extreme events, and the validity of the comparison is also limited as the convection at 6 km resolution is largely unresolved. Thereby, comparing the spatial precipitation distribution for additional extreme events and by a comparison to RACMO at improved resolution (e.g. 2.5 km resolution as in HARMONIE) is recommended as future research. Furthermore, a validation of convection-related quantities such as updraft velocity and convective available potential energy (CAPE) within extreme precipitating systems is also recommended, to assess the ability of the parameterized convection in RACMO to capture convective properties during extreme precipitation events. This should be evaluated both statistically and dynamically, and for updraft velocity the dynamical assessment should ideally include the time evolution of vertical profiles of updraft velocity (CAPE is already based on vertical profiles of temperature and specific humidity). Additionally, to assess the extent to which the spatial precipitation patterns in RACMO are misrepresented, an additional comparison to observations such as radar, satellite and station data is recommended as future research. This validation would also benefit from a quantitative assessment of spatial precipitation distribution by using a clustering index for convective organization (e.g., Tompkins and Semie, 2017).

This report is limited to the discussion of hourly precipitation extremes, and as mentioned daily precipitation extremes have already been assessed on sub-catchment scale in the Meuse by van Voorst and van den Brink (2023). However, the validation of precipitation extremes in RACMO should ideally also include a verification of return periods on other time scales, such as 6- and 12-hourly precipitation. These may show very different discrepancies compared to HARMONIE and/or observations, and are relevant for the flooding of larger basins that respond on slower time scales (but faster than daily). Additionally, we recommend assessing return periods of hourly precipitation extremes on larger spatial scales by aggregating multiple grid points (e.g. 5 by 5) in the analysis of hourly precipitation extremes. This will give an indication on the effect of the high degree of precipitation clustering in RACMO on the return periods (or other statistics) of extreme hourly precipitation events.

Chapter 5

Appendix

In this chapter, return period figures of hourly precipitation and dew point temperature for data that is pooled (see section 2.2) over the red domain in Fig. 5.1 are shown in Fig. 5.2, 5.3 and 5.4. We note that the included domain in these return period figures for RACMO from the KNMI-14 and KNMI-23 scenarios differs from RACMO reanalysis, HARMONIE and HARMONIE regridded, primarily in not including Great-Britain. Additional figures on the timing of the largest annual hourly precipitation extremes in RACMO and HARMONIE are shown in Fig. 5.5, and four time steps of a prolonged hourly extreme event in RACMO is shown in Fig. 5.6.

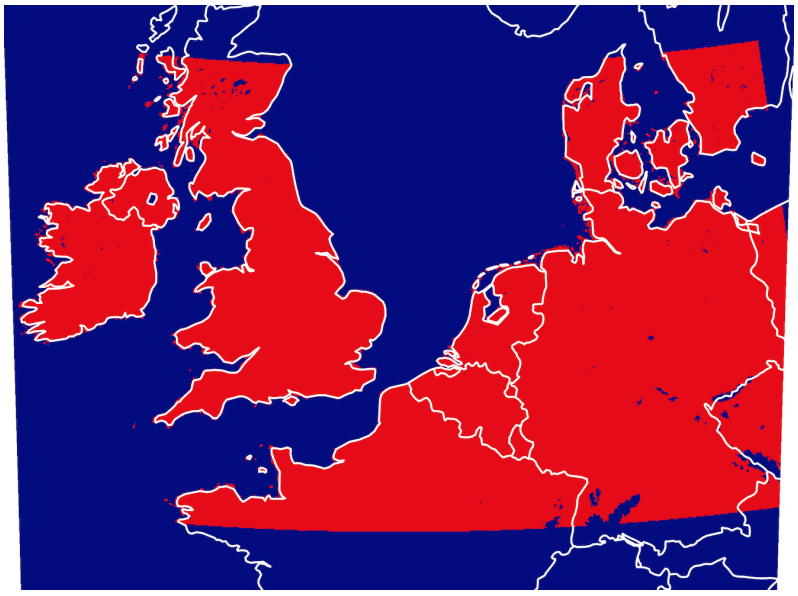

FIGURE 5.1: Map showing the domain that is adopted for data pulling of the model-comparison return period figures in appendix Fig. 5.2, 5.3 and 5.4 and in determining the largest hourly extreme events in RACMO that are shown Fig. 3.2, 3.3 and 3.3. Red indicates the grids that have been included in the analysis. The regions that are not included are either dominated by water surfaces (sea, lakes, rivers etc) or surfaces with an altitude of 700 m above sea level, or are too far north or south, thereby being subjected to very different climates.

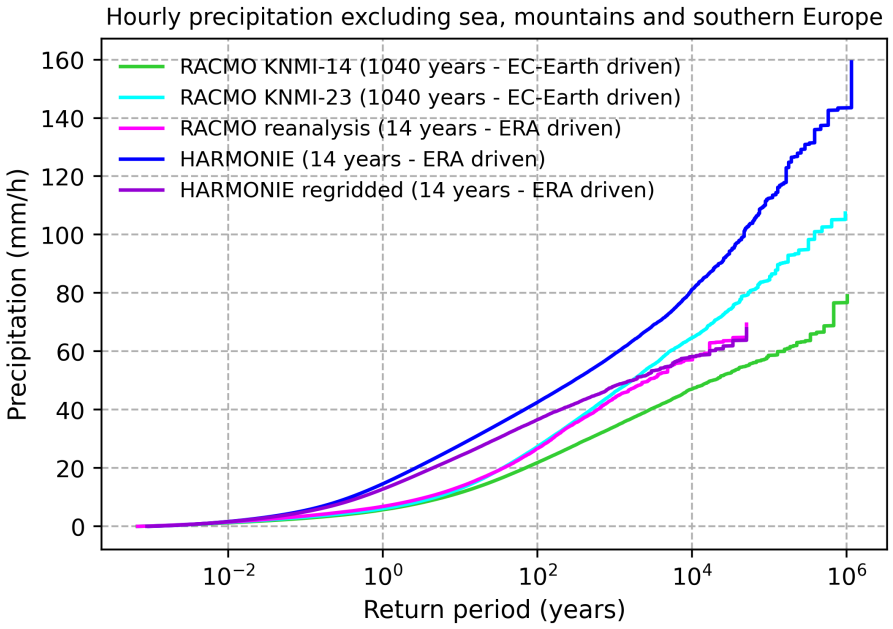

FIGURE 5.2: The return period of hourly precipitation for the domain shown in Fig. 5.1 between 2008-2021 for RACMO reanalysis (magenta), HARMONIE (blue), HARMONIE regridded (purple) forced with ERA, and for 16 ensemble members between 1949-2013 for RACMO from the KNMI-14 scenarios (green) and 16 ensemble members from 1952-2020 for RACMO from the KNMI-23 scenarios (cyan) both forced with EC-Earth, and finally for station observation data between 1991 and mid-2024 (black). We note that the included domain in this figure for RACMO from the KNMI-14 and KNMI-23 scenarios differs from RACMO reanalysis, HARMONIE and HARMONIE regridded, primarily in not including Great-Britain.

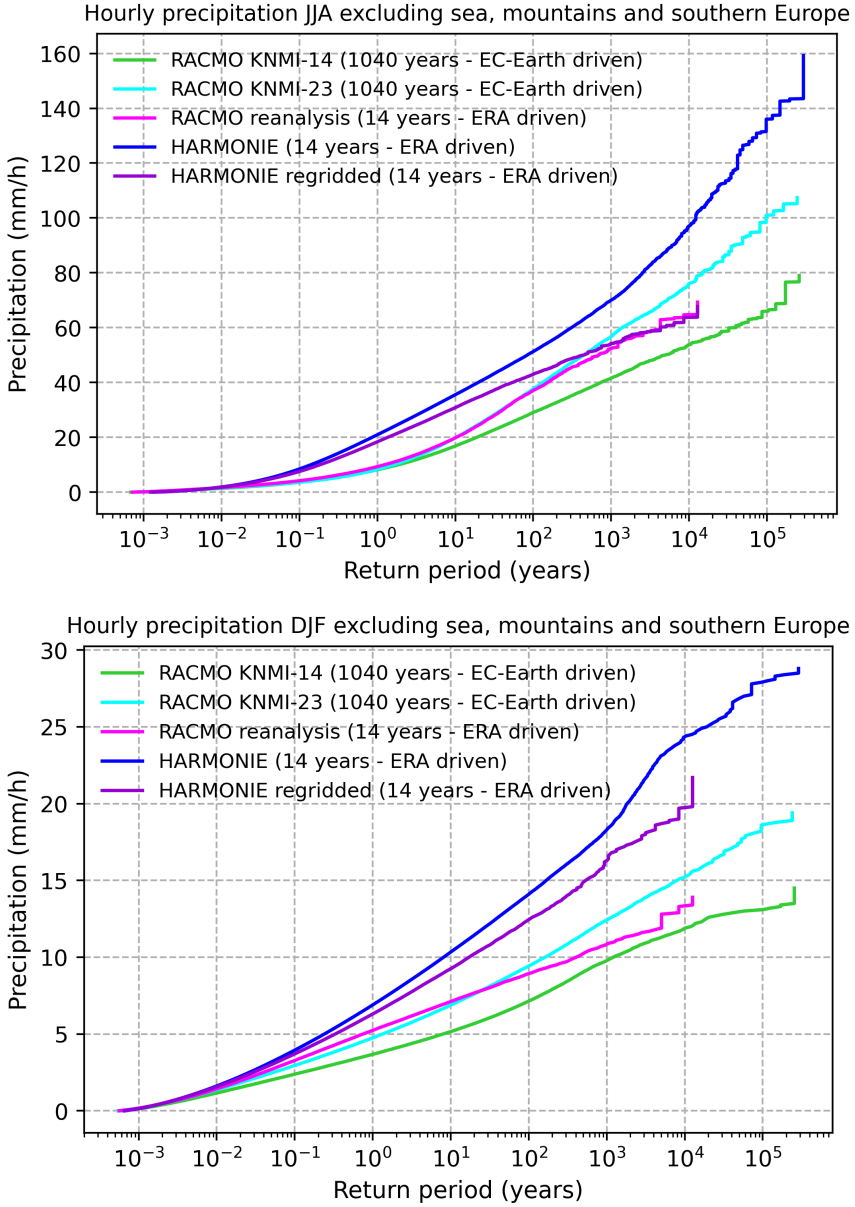

FIGURE 5.3: The return period of hourly precipitation for the domain shown in Fig. 5.1 during June, July and August (JJA, left panel) and December, January and February (DJF, right panel) between 2008-2021 for RACMO reanalysis (magenta), HARMONIE (blue), HARMONIE regridded (purple) forced with ERA, and for 16 ensemble members between 1949-2013 for RACMO from the KNMI-14 scenarios (green) and 16 ensemble members from 1952-2020 for RACMO from the KNMI-23 scenarios (cyan) both forced with EC-Earth, and finally for station observation data between 1991 and mid-2024 (black). We note that the included domain in this figure for RACMO from the KNMI-14 and KNMI-23 scenarios differs from RACMO reanalysis, HARMONIE and HARMONIE regridded, primarily in not including Great-Britain.

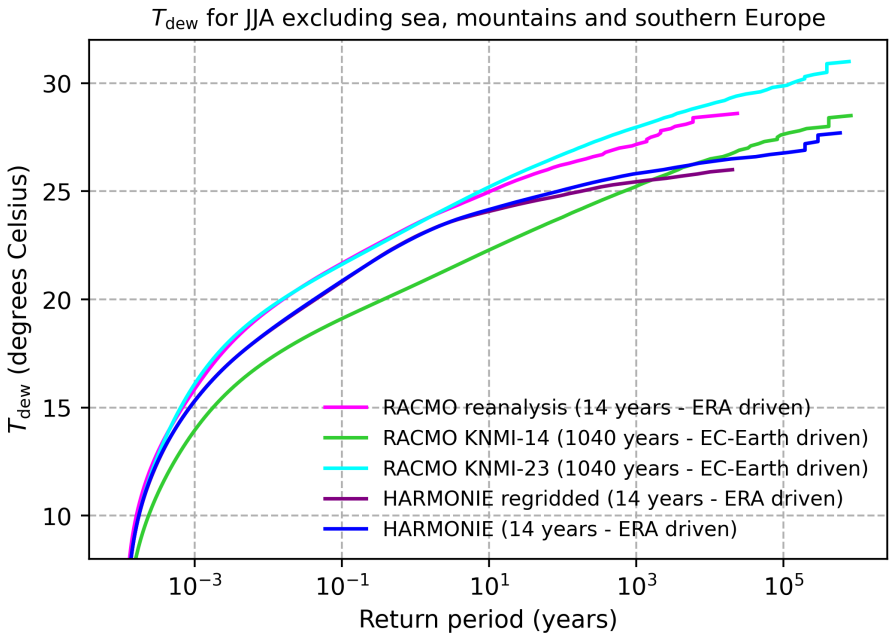

FIGURE 5.4: The return period of dew point temperature (T_{dew}) during June, July and August (JJA) for the domain shown in Fig. 5.1 between 2008-2021 for RACMO reanalysis (magenta), HARMONIE (blue), HARMONIE regridded (purple) forced with ERA, and for 16 ensemble members between 1949-2013 for RACMO from the KNMI-14 scenarios (green) and 16 ensemble members from 1952-2020 for RACMO from the KNMI-23 scenarios (cyan) both forced with EC-Earth, and finally for station observation data between 1991 and mid-2024 (black). We note that the included domain in this figure for RACMO from the KNMI-14 and KNMI-23 scenarios differs from RACMO reanalysis, HARMONIE and HARMONIE regridded, primarily in not including Great-Britain.

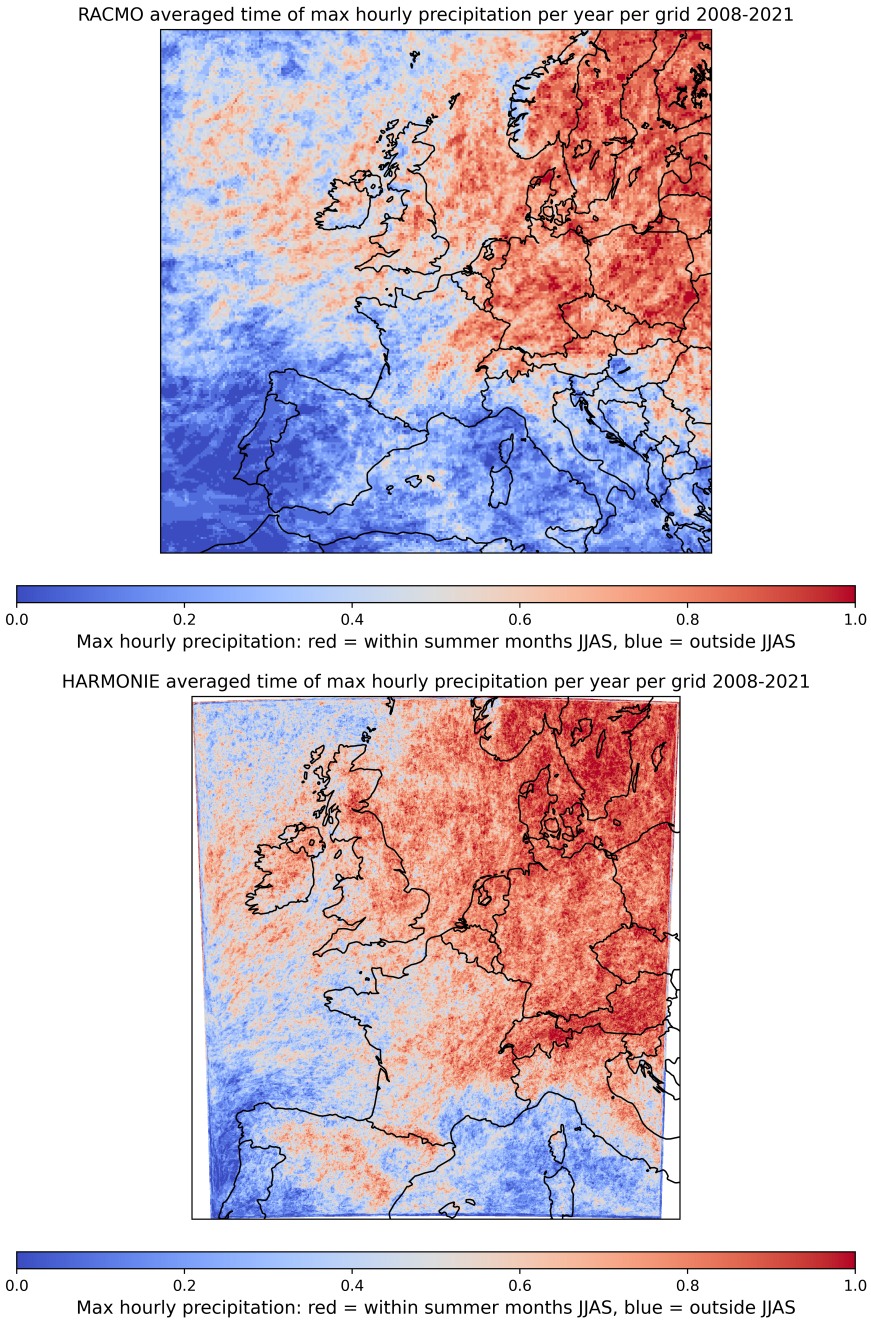

FIGURE 5.5: Index between 0 and 1 that indicates the fraction of the maximum annual hourly precipitation extremes per grid that occurred within June, July, August or September (JJAS) or outside this period between 2008-2021. If the annual maximum hourly precipitation occurred within JJAS, a 1 is assigned to the corresponding grid and otherwise a 0, and subsequently the average over the 14-year period is determined. Thereby, red regions indicate that the maximum annual hourly precipitation primarily occur during JJAS, and blue regions outside of this period.

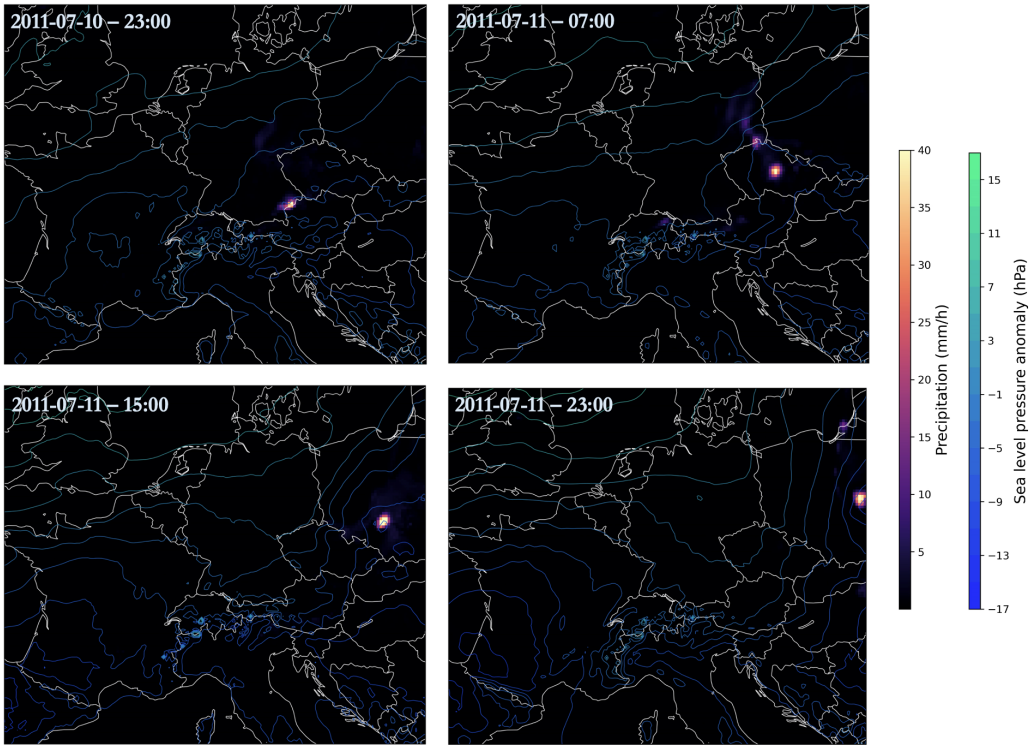

FIGURE 5.6: Four time steps of the second largest hourly extreme precipitation event in RACMO, shown at 23:00, 7:00, 15:00 and 23:00 UTC. The contours represent the sea level pressure (SLP) anomaly, given by the SLP subtracted by the yearly-averaged SLP. The event is composed of an aggregated system with large precipitation rates ($\gtrsim$30 mm/h) that persists for more than 24 hours. It eventually moves out of the RACMO domain, therefore the precise length of the event is unclear.

Bibliography

[1] Jisk Attema et al. "KNMI'14: Climate Change scenarios for the 21st Century–A Netherlands perspective". In: *KNMI: De Bilt, The Netherlands* (2014).

[2] Jisk J Attema, Jessica M Loriaux, and Geert Lenderink. "Extreme precipitation response to climate perturbations in an atmospheric mesoscale model". In: *Environmental research letters* 9.1 (2014), p. 014003.

[3] Jules Beersma, Rudolf Versteeg, and Hans Hakvoort. *Neerslagstatistieken voor korte duren: actualisatie 2018*. STOWA, 2018.

[4] Danijel Belušić et al. "HCLIM38: a flexible regional climate model applicable for different climate zones from coarse to convection-permitting scales". In: *Geoscientific Model Development* 13.3 (2020), pp. 1311–1333.

[5] Paul Berrisford et al. "The ERA-interim archive". In: *ERA report series* 1 (2009), pp. 1–16.

[6] Ralf Döscher et al. "The EC-earth3 Earth system model for the climate model intercomparison project 6". In: *Geoscientific Model Development Discussions* 2021 (2021), pp. 1–90.

[7] ECMWF. *IFS Documentation CY33R1 - Part IV: Physical Processes.* Tech. rep. 2009. DOI: 10.21957/8o7vwlbdr. URL: https://www.ecmwf.int/en/elibrary/74344-ifs-documentation-cy33r1-part-iv-physical-processes.

[8] W Hazeleger et al. "EC-Earth V2. 2: description and validation of a new seamless earth system prediction model". In: *Climate dynamics* 39 (2012), pp. 2611–2629.

[9] Hans Hersbach et al. "The ERA5 global reanalysis". In: *Quarterly Journal of the Royal Meteorological Society* 146.730 (2020), pp. 1999–2049.

[10] Elizabeth J Kendon et al. "Robustness of future changes in local precipitation extremes". In: *Journal of climate* 21.17 (2008), pp. 4280–4297.

[11] Frank Kreienkamp et al. "Rapid attribution of heavy rainfall events leading to the severe flooding in Western Europe during July 2021". In: *World Weather Atribution* (2021).

[12] Mark G Lawrence. "The relationship between relative humidity and the dewpoint temperature in moist air: A simple conversion and applications". In: *Bulletin of the American Meteorological Society* 86.2 (2005), pp. 225–234.

[13] G Lenderink et al. "Scaling and trends of hourly precipitation extremes in two different climate zones–Hong Kong and the Netherlands". In: *Hydrology and Earth System Sciences* 15.9 (2011), pp. 3033–3041.

[14] Geert Lenderink and Erik Van Meijgaard. "Increase in hourly precipitation extremes beyond expectations from temperature changes". In: *Nature Geoscience* 1.8 (2008), pp. 511–514.

[15] Geert Lenderink et al. "Scaling and responses of extreme hourly precipitation in three climate experiments with a convection-permitting model". In: *Philosophical Transactions of the Royal Society A* 379.2195 (2021), p. 20190544.

[16] Lorenzo Marchi et al. "Characterisation of selected extreme flash floods in Europe and implications for flood risk management". In: *Journal of Hydrology* 394.1-2 (2010), pp. 118–133.

[17] Judith Meyer et al. "More frequent flash flood events and extreme precipitation favouring atmospheric conditions in temperate regions of Europe". In: *Hydrology and Earth System Sciences Discussions* 2021 (2021), pp. 1–28.

[18] A Overeem et al. "Extreme value modeling of areal rainfall from weather radar". In: *Water Resources Research* 46.9 (2010).

[19] Dominik Paprotny et al. "Merging modelled and reported flood impacts in Europe in a combined flood event catalogue for 1950–2020". In: *Hydrology and Earth System Sciences* 28.17 (2024), pp. 3983–4010.

[20] V. Ruiz-Villanueva et al. "Extreme flood response to short-duration convective rainfall in South-West Germany". In: *Hydrology and Earth System Sciences* 16.5 (2012), pp. 1543–1559. DOI: 10.5194/hess-16-1543-2012. URL: https://hess.copernicus.org/articles/16/1543/2012/.

[21] Uwe Schulzweida, Luis Kornblueh, and Ralf Quast. *CDO user guide*. 2019.

[22] Adrian M Tompkins and Addisu G Semie. "Organization of tropical convection in low vertical wind shears: Role of updraft entrainment". In: *Journal of Advances in Modeling Earth Systems* 9.2 (2017), pp. 1046–1068.

[23] R Van Dorland et al. "KNMI national climate scenarios 2023 for The Netherlands". In: *KNMI: De Bilt, The Netherlands* (2023).

[24] Erik van Meijgaard et al. *The KNMI regional atmospheric climate model RACMO, version 2.1*. KNMI De Bilt, The Netherlands, 2008.

[25] Leon van Voorst and Henk van den Brink. *An evaluation of the use of regional climate model data applied to extreme precipitation in the Meuse basin*. Tech. rep. TR-413. KNMI, 2023. URL: https://www.knmi.nl/research/publications/an-evaluation-of-the-use-of-regional-climate-model-data-applied-to-extreme-precipitation-in-the-meuse-basin.

[26] Kun Xie et al. "Enhanced Evaluation of Sub-daily and Daily Extreme Precipitation in Norway from Convection-Permitting Models at Regional and Local Scales". In: *Hydrology and Earth System Sciences Discussions* 2024 (2024), pp. 1–38.

Royal Netherlands Meteorological Institute

PO Box 201 | NL-3730 AE De Bilt
Netherlands | www.knmi.nl